Photoinduced Electron Transfer from Nitoxide Free Radicals to the Triplet State of C_{60}

Yasuyuki Araki,[†] Hongxia Luo,[†] Shafiqul D.-M. Islam,[†] Osamu Ito,*[,†] Michio M. Matsushita,[‡,§] and Tomokazu Iyoda[‡,||]

Institute of Multidisciplinary Research for Advanced Materials, Tohoku University, CREST, (JST), Katahira, Aoba-ku, Sendai 980-8577, and Department of Applied Chemistry, Graduate School of Engineering, Tokyo Metropolitan University, Minami-Ohsawa, Hachioji, Tokyo 192-0397, Japan

Received: October 29, 2002; In Final Form: February 22, 2003

The photoinduced electron transfer of C_{60} in the presence of stable free radicals such as nitoxides has been studied by nanosecond laser photolysis by measuring the transient absorption spectra in the visible and near-IR regions. For the *N*-oxy-piperidine radical, the rise of the radical anion of C_{60} was not observed, although the decay rate of the triplet excited state of C_{60} was quite fast. For free radicals with 4,4,5,5-tetramethylimidazoline-1-oxyl-3-oxide (nitronyl nitroxide), electron transfer via the triplet excited state of C_{60} was confirmed from the rise of the anion radical of C_{60}, although the quantum yield of electron transfer is not high. From the rates and efficiencies of electron transfer, which are strongly affected by the donor ability of the substituents on the phenyl moiety of the nitronyl nitroxide radical, a specific spin−spin interaction of the triplet spin state of C_{60} with the doublet spin state of the nitronyl nitroxide radical was revealed. In the longer time scale measurements, the radical anion of C_{60} persisted for a long time, suggesting that the nitronyl nitoxide cation, which was formed by donating an electron to the triplet state of C_{60}, forms the complex with the nitronyl nitoxide radical. An electron-mediating process from the radical anion of C_{60} to the viologen dication was confirmed by the rise of the radical cation of the viologen, with the concomitant decay of the radical anion of C_{60}. Final back electron transfer from the viologen radical cation to the nitronyl nitroxide cation was observed by the transient absorption measurements on additional long time scales.

Introduction

It has been pointed out that the triplet states of fullerenes act as good electron acceptors in the photoinduced electron-transfer processes in mixture systems with electron donors in polar solvents.[1−3] Because of the high delocalization of the π electrons in fullerenes, the transient absorption bands due to the excited singlet states, triplet states, and radical anions appear in the visible and near-IR regions.[4,5] As electron donors, aromatic amines,[6,7] tetrathiafulvalenes,[8] and porphyrins/phthalocyanines[9] were employed for a decade; these compounds were proven to donate the electron efficiently toward the triplet states of fullerenes. However, little research has been reported on electron transfer from free radicals (FR) to fullerenes (C_{60} and C_{70}) under photoillumination. Samanta and Kamat reported that the triplet states of C_{60} ($^3C_{60}^*$) and C_{70} ($^3C_{70}^*$) were quenched efficiently with the nitroxide free radicals in methylene chloride, but the formation of the radical anions of C_{60} and C_{70} ($C_{60}^{\bullet-}$ and $C_{70}^{\bullet-}$) was not confirmed;[10] thus, they postulated appreciable spin−spin interactions between $^3C_{60}^*$ or $^3C_{70}^*$ and the nitoxide free radicals.[11] To confirm the electron transfer from the free radicals, it is necessary to employ free radicals with stronger donor ability than the simple nitoxide free radicals. Furthermore, it is indispensable to detect the rise of $C_{60}^{\bullet-}$ and $C_{70}^{\bullet-}$ in the presence of free radicals upon measuring the transient spectra in the visible and near-IR regions, which permitted us to confirm photoinduced electron transfer, giving quantitative consideration to the spin−spin interactions.

In the present study, we employed the nitroxide radical (TEMPO; **1**) and the nitronyl nitroxide radicals (**2**−**4**) as shown in Scheme 1 in which **1** is common to the study by Samanta and Kamat.[10] It is expected that nitronyl nitroxide radicals **2**−**4** may have higher electron donor abilities in which the *N*-dimethylamine moiety on the phenyl group in **4** may further increase the donor ability more than the hydroxy substituents in **2** and **3**.

We report here that the efficiencies and rates of photoinduced electron transfer can be easily evaluated with the decay of the excited states and the rise of the radical anion of C_{60} in the presence of these free radicals by measuring the transient absorption spectra in the visible and near-IR regions. The rates and quantum yields for electron transfer via $^3C_{60}^*$ were compared by changing the structures of the free radicals to reveal spin−spin interactions between the triplet spin state of C_{60} and the doublet spin state of the free radicals.

Furthermore, we investigated the addition effect of the viologen dication; in such systems, $C_{60}^{\bullet-}$ can mediate its electron transfer to the viologen dication. This reveals that the photosensitizing electron-transfer/electron-mediating system will be established under photoexcitation of the fullerenes in the presence of the free radicals and viologen dication.

Experimental Section

Materials. C_{60} was obtained from the Texas Fullerenes Corporation at a purity of 99.9%. TEMPO (**1**) was commercially

* To whom correspondence should be addressed. E-mail: ito@tagen.tohoku.ac.jp. Fax: +81-22-217-5608.

[†] Tohoku University.

[‡] Tokyo Metropolitan University.

[§] Present address: Graduate School of Arts and Sciences, The University of Tokyo, Tokyo, Japan.

[||] Present address: Chemical Resources Laboratory, Tokyo Institute of Technology, Tokyo, Japan.

10.1021/jp0273373 CCC: $25.00
Published on Web 04/01/2003

SCHEME 1

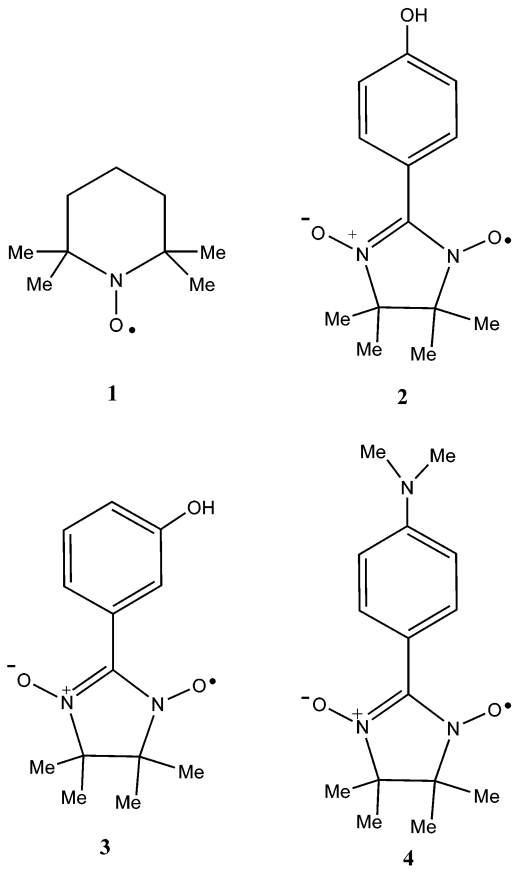

available; nitronyl nitroxides (**2**−**4**) were prepared by the method reported in the literature.[12] Perchlorate of octyl viologen dication (OV^{2+}) was used as a second electron acceptor for the electron-mediating system. Benzonitrile (PhCN) used as a solvent was of HPLC grade.

Apparatus. Oxidation potentials (E_{ox}) of **1**−**4** were measured by a voltammetric analyzer (BASCV-50W) in a conventional three-electrode cell equipped with Pt working- and counter-electrodes with an Ag/AgCl reference electrode in the presence of ferrocene as an internal standard. In each case, solutions contained 1.0−5.0 mmols of the sample and 0.1 mols of tetrabutylammonium perchlorate (Nakalai Tesque); the solution was deaerated with Ar bubbling before measurements.

Steady-state absorption spectra were measured with a JASCO/V-570 spectrophotometer. Transient absorption spectra in the visible and near-IR regions were observed by the laser-flash photolysis apparatus. In the systems of C_{60}^- free radicals and C_{60}^- free radicals−OV^{2+}, C_{60} was excited with the SHG (532-nm) light of a Nd:YAG laser (Quanta-Ray; 6 ns fwhm). For measurements shorter than 5 μs, a Si-PIN photodiode module (400−600 nm) and a Ge-APD module (600−1600 nm) were employed as detectors for monitoring the light from a pulsed Xe lamp.[13,14] For measurements longer than 5 μs, an InGaAs-PIN photodiode was used as a detector for monitoring light from continuous Xe-lamp (150 W).[14,15] The sample solutions were deaerated by Ar bubbling before measurements. Laser photolysis was performed for the solution in a rectangular quartz cell with a 10-mm optical path. All of the measurements were carried out at 23 °C.

Molecular Orbital Calculation. The optimized structures, energy levels, and unpaired electron densities of the free radicals were calculated via Gaussian 98 at the B3LYP/6-31+G(d) level.

TABLE 1: E_{ox} and E_{SOMO} of FRs, $\Delta G°_{et}$ for Electron Transfer from FRs to $^3C_{60}$*, and $\Delta G°_{bet}$ for Back Electron Transfer from $C_{60}^{\bullet-}$ to FR^+s

	E_{ox}/V[a]	E_{SOMO}/eV	$\Delta G°_{et}$/eV	$\Delta G°_{bet}$/eV
1	0.22	−6.03	−0.45	−1.08
2	0.24	−4.81	−0.43	−1.10
3	0.30	−4.99	−0.37	−1.16
4	0.16	−4.60	−0.51	−1.02
DMA[b]	0.53		−0.14	−1.39

[a] Versus ferrocene/ferrocene$^+$. [b] DMA (dimethylaniline).

Results and Discussion

Cyclic Voltammetry. Cyclic voltammograms show the reversible curves for all free radicals. The oxidation potential (E_{ox}) of **1** is in good agreement with the reported value.[14] The measured E_{ox} values are listed in Table 1. The order of E_{ox} is **3** > **2** > **1** > **4**. The free radicals with less positive E_{ox} values have higher donor abilities; thus, the order of the donor ability is **4** > **1** > **2** > **3**. The free-energy changes for electron transfer ($\Delta G°_{et}$) from the free radicals (FR) to $^3C_{60}^*$ can be calculated by the Rehm−Weller equation.[15]

$$\Delta G°_{et} = E_{ox}(FR) - E_{red}(C_{60}) - E_T(C_{60}) - E_c \qquad (1)$$

$E_{red}(C_{60})$ is the reduction potential (= −0.92 V vs ferrocene/ferrocene$^+$ in PhCN),[16] $E_T(C_{60})$ is the T_1 energy levels (= 1.53 eV),[17] and E_c is the Coulomb energy (0.06 eV in PhCN).[6] Thus, the $\Delta G°_{et}$ values were obtained as listed in Table 1. A sufficiently negative $\Delta G°_{et}$ value predicts the diffusion-controlled second-order rate constants for the electron-transfer process via $^3C_{60}^*$ in PhCN.

Molecular Orbital Calculations. MO patterns of the SOMOs of **1**−**4** are shown in Figure 1. The electron in SOMO is localized mainly on the N−O moieties. The energy levels of the SOMOs are summarized in Table 1; the increasing order of the SOMO levels for the nitronyl nitroxide radicals is **4** > **2** > **3**, which is in good agreement with the E_{ox} values. The HOMOs for **2**−**4** are localized on the phenol and dimethyaniline (DMA) moieties (Supporting Information). Even in **4**, the energy level of the SOMO localized on the N−O moieties is higher than that of the HOMO localized on the DMA moiety, supporting a smaller E_{ox} value of **4** than that of DMA in Table 1, which predicts that the donor ability of **4** is higher than that of DMA. In the case of **1**, a large E_{ox} value would be anticipated from the low SOMO level whereas the E_{ox} value of **1** is smaller than those of **2** and **3** probably because of the low precision of the MO calculations for different series of structures.

Steady-State Absorption Spectra. The steady-state absorption spectra of **1**−**4** are shown in Figure 2. Nitroxide radical **1** shows weak absorption in the visible region (400−500 nm) but intense absorption at shorter wavelengths than 300 nm. Nitronyl nitroxide radicals **2**−**4** show intense absorption in the visible region (550−700 nm) and strong absorption at wavelengths shorter than 430 nm. The absorption spectrum of C_{60} also extends to wide visible and UV regions (Figure 2). The spectra of the mixtures of C_{60} with each of the compounds **1**−**4** in PhCN are almost the same as the calculated spectra that are produced by adding the absorption bands of C_{60} and **1**−**4**, suggesting that no appreciable interaction exists between C_{60} and **1**−**4** in the ground state. From the absorption spectra in Figure 2, the laser light at 532 nm excites both C_{60} and **2**−**4**; however, no appreciable transient absorption band appeared by the excitation of only **2**−**4** with the 532-nm laser light. Therefore, we could obtain the photoinduced processes via the excited states of C_{60} employing the 532-nm laser light.

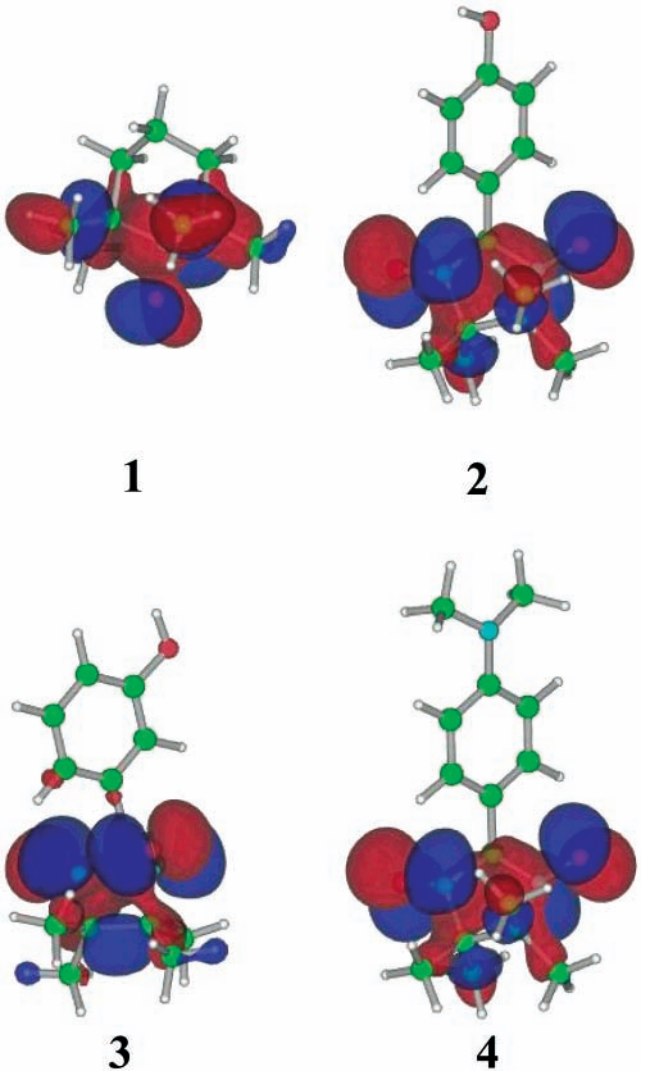

Figure 1. Unpaired electron distributions of the SOMO of free radicals.

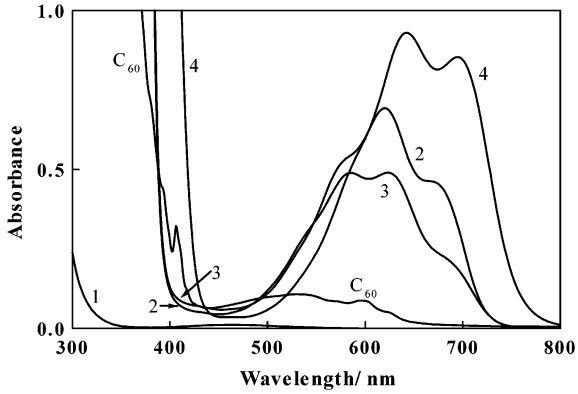

Figure 2. Steady-state absorption spectra of C_{60} (0.1 mM) and **1**−**4** (0.1 mM) in PhCN.

Nanosecond Transient Absorption Spectra. Figure 3 shows the nanosecond transient spectra in the visible and near-IR regions observed via laser excitation of C_{60} with 532-nm light in the presence of **1** in PhCN. The 740-nm band was attributed to $^3C_{60}$*, which is produced via intersystem crossing (ISC) from the singlet excited state ($^1C_{60}$*) immediately after the nanosecond laser pulse.[18] The increase in the decay rates of $^3C_{60}$* was observed on addition of **1**, but the absorption band due to $C_{60}^{\bullet-}$ was not observed in the near-IR region, suggesting that electron transfer producing the solvated radical ions or solvent-separated ion pair does not take place. The calculated ΔG°_{et} is negative for **1**, predicting that electron transfer occurs; thus, partial electron transfer may be possible, probably via an exciplex such as ($^3(C_{60}^{\delta\bullet-}\cdots\mathbf{1}^{\delta+})$*). However, before the dissociation of the exciplex into the free-radical ions, the rapid deactivation of $^3C_{60}$* by **1** is induced within the exciplex by the spin−spin interaction between $^3C_{60}$ and the doublet spin of **1**.[11]

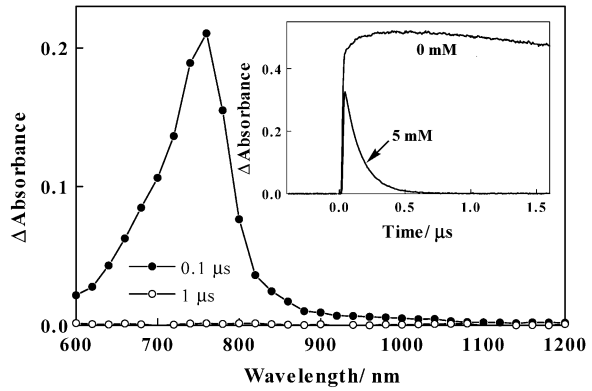

Figure 3. Transient absorption spectra obtained by 532-nm laser-light excitation of C_{60} (0.1 mM) in the presence of **1** (5 mM) in deaerated PhCN. Inset: Time profiles at 740 nm in the presence and absence of **1**.

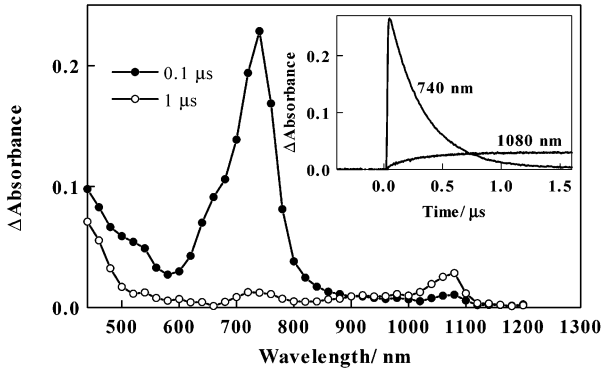

Figure 4. Transient absorption spectra obtained by 532-nm laser-light excitation of C_{60} (0.1 mM) in the presence of **4** (1 mM) in deaerated PhCN. Inset: Time profiles at 740 nm in the presence and absence of **4**.

SCHEME 2

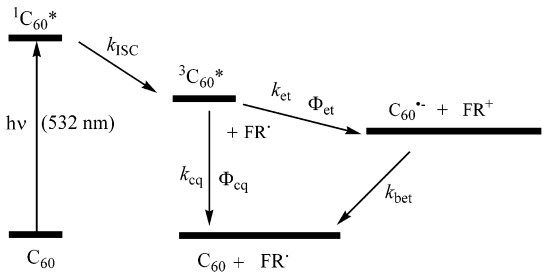

In the presence of nitronyl nitroxide radicals such as **4**, the absorption intensity of $C_{60}^{\bullet-}$ at 1080 nm[4−9] increased (Figure 4), accompanied by the decay of $^3C_{60}$*, suggesting that $C_{60}^{\bullet-}$ is formed via $^3C_{60}$* accepting an electron from **4**.

The time profiles for the decay of $^3C_{60}$* at 740 nm and the rise of $C_{60}^{\bullet-}$ at 1080 nm are shown in the inset of Figure 4 in the presence of **4**. The decay curve of $^3C_{60}$* and the rising curve of $C_{60}^{\bullet-}$ are almost mirror images, supporting the fact that electron transfer takes place via $^3C_{60}$* as shown in Scheme 2, in which k_{ISC}, k_{et}, and k_{cq} are referred to as the rate constants of

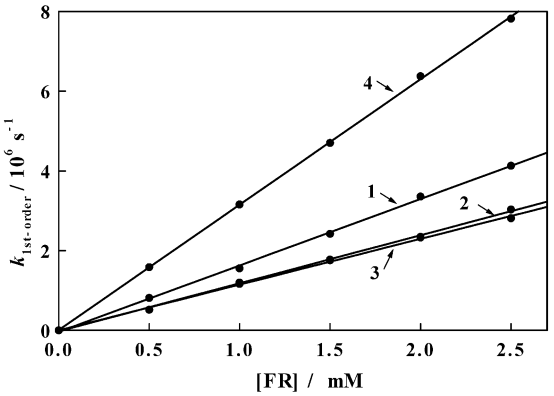

Figure 5. Pseudo-first-order plots of the decay of $^3C_{60}$* at 740 nm in the presence of various concentration of **1**−**4** in deaerated PhCN.

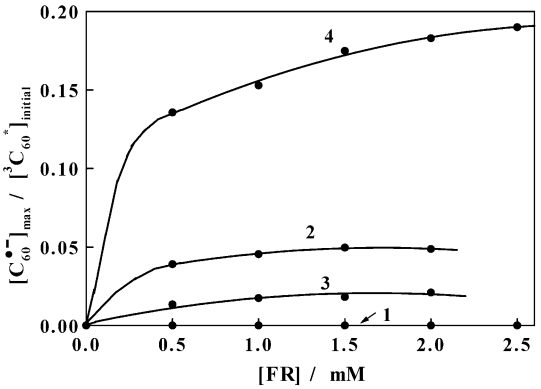

Figure 6. Dependence of efficiencies ($[C_{60}^{\bullet-}]_{max}/[^3C_{60}^*]_{initial}$) on the free-radical concentration.

TABLE 2: Evaluated Rate Parameters k_q, Φ_{et}, k_{et}, and k_{bet} in PhCN

	k_q/M^{-1} s^{-1}	Φ_{et}	k_{et}/M^{-1} s^{-1}	k_{bet}/M^{-1} s^{-1}
1	1.6×10^9	0.00		
2	1.2×10^9	0.02	2.4×10^7	
3	1.1×10^9	0.05	5.5×10^7	
4	2.6×10^9	0.20	6.2×10^8	2.6×10^9
DMA	1.4×10^9 *a*	0.69[a]	9.5×10^8 *a*	5.1×10^9 *a*

[a] Evaluated in the present study.

intersystem crossing from $^1C_{60}$* to $^3C_{60}$*, electron transfer, and collisional quenching, respectively. In the collisional quenching, the acceleration of the decay of $^3C_{60}$* by spin−spin interaction may be included. The observed slow rise of $C_{60}^{\bullet-}$ clearly indicates that electron transfer does not take place via $^1C_{60}$* because of quick intersystem crossing (ISC) from $^1C_{60}$* to $^3C_{60}$* (0.8×10^9 s^{-1}).[19] In the cases of **2** and **3**, similar transient absorption spectral changes and time profiles were observed; however, the absorption intensities of $C_{60}^{\bullet-}$ were smaller that those from the $^3C_{60}$*−**4** system.

Quantum Yields and Rates for Electron Transfer. Each decay of $^3C_{60}$* at 740 nm obeys first-order kinetics, yielding the first-order rate constant ($k_{first-order}$). The $k_{first-order}$ value increases linearly with the concentration of the free radicals. The second-order quenching rate constants (k_q) for $^3C_{60}$* quenched by the free radicals can be obtained from the linear slopes of the pseudo-first-order plots as shown in Figure 5. The k_q values are listed in Table 2. All of the free radicals (**1**−**4**) have k_q values in the range of $(0.75-2.6) \times 10^9$ M^{-1} s^{-1}.

The efficiency of electron transfer via $^3C_{60}$* can be obtained from the ratio of the maximum absorbance of $C_{60}^{\bullet-}$ at 1080 nm to the initial maximum absorbance of $^3C_{60}$* at 740 nm, $[C_{60}^{\bullet-}]_{max}/[^3C_{60}^*]_{int}$.[20] The ratios show the saturation upon increasing the concentration of the free radicals, as shown in Figure 6.[19,20] At sufficiently high concentrations of the free radicals above ca. 3 mM, the efficiency can be set equal to the quantum yield (Φ_{et}) of the electron-transfer process via $^3C_{60}$* (Table 2). Since all Φ_{et} values in Table 2 are less than 1.0, there may be quenching processes other than electron transfer. Finally, the electron-transfer rate constants (k_{et}) are obtained from $k_{et} = \Phi_{et}k_q$ as listed in Table 2.[20] The k_{et} values are considerably smaller than the diffusion-controlled limit ($k_{diff} = 5.2 \times 10^9$ M^{-1} s^{-1} in PhCN),[21] although the $\Delta G°_{et}$ values calculated from the Rehm−Weller equation are all sufficiently negative (Table 1) to predict the diffusion-controlled second-order rate constants for the electron-transfer processes.

Since the $^3C_{60}$*−phenol system does not show any decay of $^3C_{60}$* in PhCN, no electron transfer occurs.[22] Compared with phenol, **2** and **3** show very large k_q values and finite k_{et} and Φ_{et} values, which is ascribed to the moderately high donor ability of the nitonyl nitoxide moiety. Compared with k_q, k_{et}, and Φ_{et} of the $^3C_{60}$*−dimethylaniline (DMA) system (Table 2), the Φ_{et} and k_{et} values of **4** are small, although the k_q value is large. One of the typical triplet quenching mechanisms is energy transfer; however, the energy-transfer process from $^3C_{60}^*$ to **1**−**4** may be neglected because the energy level of $^3C_{60}^*$(1.53 eV) lies lower than the lowest excited doublet state of **1**−**4** (>1.7 eV), which can be evaluated from the fluorescence spectra as shown in the Supporting Information.

These findings clearly suggest some specific spin−spin interaction between $^3C_{60}$* and **4**. Such interaction was also found between $^3C_{60}$* and **1**, where no electron transfer occurs; nevertheless, efficient quenching ($k_q = 1.6 \times 10^9$ dm^3 mol^{-1} s^{-1} in PhCN) and sufficiently negative $\Delta G°_{et}$ values (Table 1) resulted.

These observations suggest the specific spin−spin interaction that can be described as collisional quenching processes in Scheme 2. Such spin−spin interaction may be interpreted by enhanced ISC process (EIP) from $^3C_{60}^*$ to its ground state by the paramagnetism of **1**−**4**.[11a−h]

The rate of the EIP can be estimated from eq 1:[11a−c]

$$k_{EIP} = \frac{4\pi^2|H_{ex}|^2F}{hH_\nu} \qquad (2)$$

H_{ex} is the exchange interaction matrix element for the encounter of the triplet-state molecules with paramagnetic species, H_ν is the density of the final vibration energy states (after quenching), and h is Plank's constant. The Franck−Condon factor, F, can be given by eq 3, assuming that the F value for $^3C_{60}^*$ is almost the same as for ordinal aromatic carbon:[11a]

$$F = 0.15 \exp\left\{\frac{-\Delta E - 4000}{2175}\right\} \qquad (3)$$

ΔE is the energy (cm^{-1}) between the triplet and the ground state. The ΔE value for C_{60} was calculated to be 12 200 cm^{-1}, which results in $F = 8.7 \times 10^{-5}$ cm^{-1}. Assuming that H_{ex} and H_ν are 50 cm^{-1} [11b] and 30 cm^{-1},[11g] respectively, the k_{EIP} value was finally evaluated to be 8.6×10^9 s^{-1}. This rate is much faster than the inverse of the lifetime of $^3C_{60}^*$ in the solution (ca. 5×10^4 s^{-1}).[6,8,20] Blank et al. also estimated the encounter

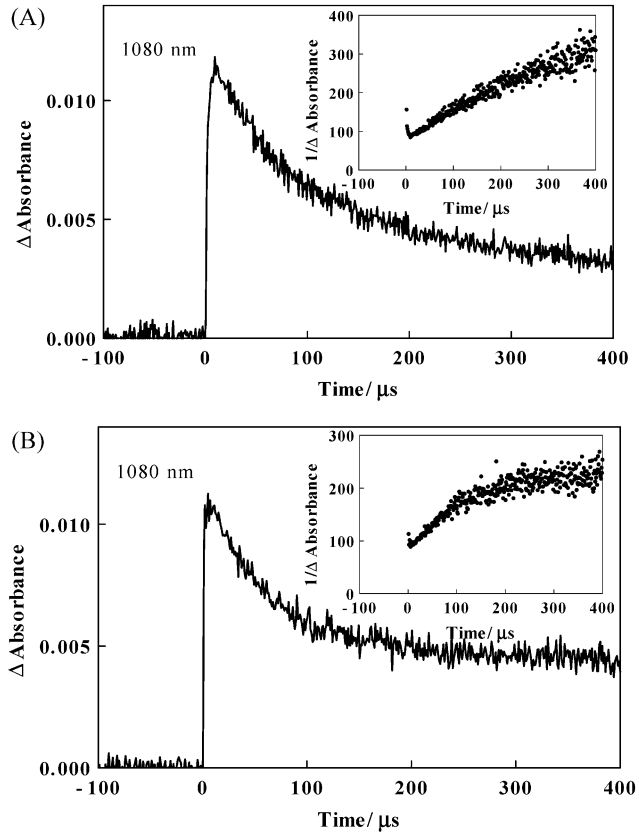

Figure 7. Long time scale decay of $C_{60}^{\bullet-}$ produced by electron transfer from **4** in deaerated PhCN (at 1080 nm). (A) Low concentration of **4** (0.3 mM), and (B) high concentration of **4** (1 mM). Inset: Second-order plots.

time (τ) between the triplet-state molecule and the doublet-state radicals by employing eq 4:[11g]

$$\tau \approx \frac{(R_e)^2}{D} \tag{4}$$

R_e is the distance between the center of $^3C_{60}^*$ and FR in the encounter complex, and D is the mutual diffusion coefficient. If the τ value is comparable to $1/k_{EIP}$ (1.2×10^{-10} s), then $^3C_{60}$* is considered to interact with doublet-state radicals such as **1**−**4**. In the case of $^3C_{60}^*$ and FR, $R_e \approx 7 \times 10^{-8}$ cm was evaluated from the sum of the C_{60} radius (4 Å) and the **1**−**4** radii (3 Å). Thus, the D value can be estimated by the Stokes−Einstein relation (eq 5):

$$D = \frac{100k_BT}{6\pi\eta\left(\frac{1}{R_T} + \frac{1}{R_r}\right)} \tag{5}$$

k_B, T, η, R_T, and R_r are Boltzmann's constant, absolute temperature, solvent viscosity, radius of $^3C_{60}^*$, and radius of the radicals, respectively. The D value evaluated by eq 4 is ca. 9×10^{-6} cm^2 s^{-1}. Finally, from eq 4, the τ value was estimated to be 5×10^{-10} s, which seems to be comparable to $1/k_{ISC}$ (1.2×10^{-10} s) in PhCN. Therefore, $^3C_{60}^*$ has enough time to interact with **1**−**4** in PhCN. Consequently, we can conclude that $^3C_{60}^*$ is quenched by **1**−**4** mainly because of the EIP mechanism.

Back Electron Transfer. After reaching the maximum intensity, $C_{60}^{\bullet-}$ begins to decay as shown in Figure 7 on a longer time scale. At the low concentration of **4**, the second-order plot for the decay of $C_{60}^{\bullet-}$ shows a linear relation (inset of Figure

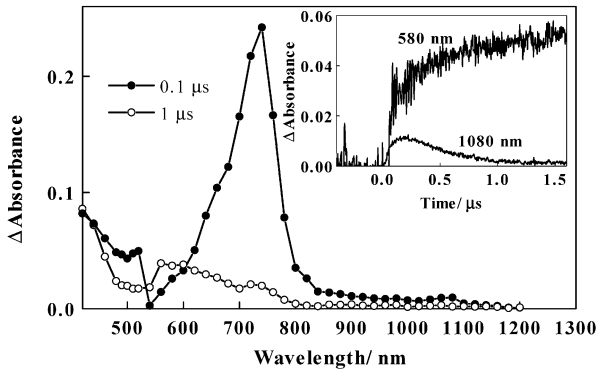

Figure 8. Transient absorption spectra obtained by 532-nm laser-light excitation of C_{60} (0.1 mM) in the presence of **4** (1 mM) and OV^{2+} (2 mM) in deaerated PhCN. Inset: Time profiles at 580 and 1080 nm.

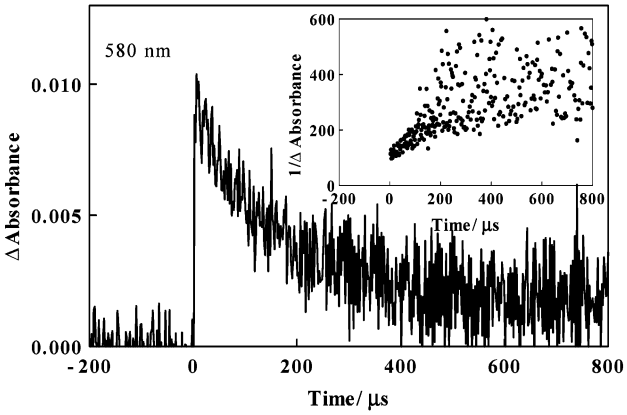

Figure 9. Long time scale decay of $OV^{\bullet+}$ in the presence of $\mathbf{4}^+$ in deaerated PhCN (at 1080 nm).

9). Observed second-order kinetics indicates the bimolecular reaction, probably due to the recombination of $C_{60}^{\bullet-}$ with FR^+, yielding a neutral molecule and a neutral radical in their ground states, respectively (Scheme 2). Bimolecular second-order kinetics also suggests that back electron transfer takes place after FR^+ and $C_{60}^{\bullet-}$ were separately solvated as a free cation and free-radical anion, respectively. The slope of the second-order plot is attributed to k_{bet}/ϵ_A, where ϵ_A is the molar extinction coefficient of $C_{60}^{\bullet-}$. On substituting the reported ϵ_A at 1080 nm for $C_{60}^{\bullet-}$,[20] the k_{bet} values were evaluated as listed in Table 2. The k_{bet} values are all quite similar to k_{diff}.[21]

Under the higher concentration of **4**, the initial part of the decay is similar to that at the low concentration of **4**, obeying the second-order kinetics and giving a similar k_{bet} value. In the later part, however, the decay slowed, showing a bent line in the second-order plot. This indicates that FR^+ changes into substance(s) having low electron-accepting ability; thus, the electron on $C_{60}^{\bullet-}$ cannot return to FR^+. The concentration effect of $\mathbf{4}^+$ invokes the formation of a dimer radical cation such as $(\mathbf{4})_2^{\bullet+}$ between $\mathbf{4}^+$ and **4**.

If $(\mathbf{4})_2^{\bullet+}$ is stable, then the accumulation of $C_{60}^{\bullet-}$ can be observed even by the steady-state irradiation of C_{60} in the presence of **4** in PhCN; the steady-state absorption spectra measured during the steady-light irradiation did not show persistent $C_{60}^{\bullet-}$ in the near-IR region (Supporting Information). This suggests that $(\mathbf{4})_2^{\bullet+}$ is not stable. However, the lifetime of $(\mathbf{4})_2^{\bullet+}$ may be longer than 2−3 ms, as evaluated from the time profile in Figure 7.

Electron-Mediating System. Figure 8 shows the transient absorption spectra observed by the laser-light excitation of the band of C_{60} in the presence of **4** and octyl viologen dication

SCHEME 3

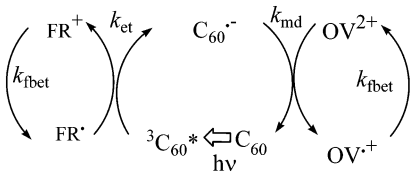

(OV^{2+}), which is a well-known electron acceptor from $C_{60}^{\bullet-}$. Accompanied by the rise and decay of $C_{60}^{\bullet-}$, $OV^{\bullet+}$ appeared at 580−600 nm.[23] These observations suggest that an electron of $C_{60}^{\bullet-}$ transfers to OV^{2+}, thus producing $OV^{\bullet+}$, which is referred to as an electron-mediating process. Thus, it is proven that the photosensitized electron-transfer/electron-mediating system was established with the photoexcitation of C_{60} as shown in Scheme 3, in which k_{md} is referred to as the rate constant of the electron-mediating process and k_{fbet} is referred to as the final back-electron-transfer process from $OV^{\bullet+}$ to FR^+ returning to OV^{2+} and FR. The k_{md} value was evaluated to be 1.5×10^9 M^{-1} s^{-1} in PhCN from the decay of $C_{60}^{\bullet-}$ (inset of Figure 8) upon changing the concentration of OV^{2+}.

The decay-time profile of $OV^{\bullet+}$ at 580 nm in the presence of $\mathbf{4}^+$ is shown in Figure 9, in which $OV^{\bullet+}$ shows almost complete decay at 800 μs. From the second-order plot for the decay of $OV^{\bullet+}$, the slope of the second-order plot of $OV^{\bullet+}$ gave $k_{fbet} = 8.2 \times 10^8$ M^{-1} s^{-1}. This finding indicates that the lifetime of $OV^{\bullet+}$ increases by a factor of ca. 3 because final back electron transfer between both positively charged species ($OV^{\bullet+}$ and FR^+) was retarded compared with back electron transfer between oppositely charged species ($C_{60}^{\bullet-}$ and FR^+).

Steady-state measurements of the system during light irradiation did not show an accumulation of $OV^{\bullet+}$ at 580 nm (Supporting Information), which is in good agreement with the time profile showing the almost complete decay of $OV^{\bullet+}$ (Figure 9). The dimer radical cation $(\mathbf{4})_2^{\bullet+}$ may be destabilized to dissociate into $\mathbf{4}^+$ and **4** in the presence of OV^{2+}. Thus, the accumulation of $OV^{\bullet+}$ was impossible. This implies that the photosensitized electron-transfer/electron-mediating system of $^3C_{60}{}^*-\mathbf{4}-OV^{2+}$ is reversible.

Summary

The transient species of C_{60} such as the triplet excited state and the radical anion were well followed by the transient absorption spectra in the visible and near-IR regions. C_{60} acts as a good photosensitizer and a good electron acceptor in the presence of the nitronyl nitroxide free radicals. Electron donor abilities of FRs are lower than expected from the oxidation potentials probably because FRs are good triplet quenchers because of the spin−spin interaction between the excited triplet spin state of C_{60} and the doublet spin state of free radicals. The concentration effect on the back-electron-transfer process suggests the formation of the dimer radical cation. On addition of a viologen dication, the reversible photosensitized electron-transfer/electron-mediating cycle was confirmed.

Acknowledgment. We are grateful for financial support from a Grant-in-Aid on Scientific Research (14050014 and 14350449) from the Ministry of Education, Culture, Sports, Science, and Technology of Japan and from the Mitsubishi Foundation.

Supporting Information Available: Cyclic voltammograms, HOMO, transient absorption spectra, fluorescence spectra, and steady-state absorption spectra during photolysis. This material is available free of charge via the Internet at http://pubs.acs.org.

References and Notes

(1) Guldi, D. M.; Kamat, P. V. *Fullerenes, Chemistry, Physics and Technology*; Kadish, K. M., Ruoff, R. S., Eds.; Wiley-Interscience: New York, 2000; pp 225−281.

(2) Maggini, M.; Guldi, D. M. *Molecular and Supramolecular Photochemistry*; Ramamurthy, V., Schanze, K. S., Eds.; Marcel Dekker: New York, 2000; Vol. 4, pp 149−196.

(3) O. Ito *Res. Chem. Intermed*. **1997**, *23*, 389.

(4) Arbogast, J. W.; Foote, C. S. *J. Am. Chem. Soc*. **1991**, *113*, 8886.

(5) Senior, R. J.; Szarka, A. Z.; Smith, G. R.; Hochstrasser, R. M. *Chem. Phys. Lett*. **1991**, *185*, 179.

(6) Arbogast, J. W.; Foote, C. S.; Kao, M. *J. Am. Chem. Soc*. **1992**, *114*, 2277.

(7) (a) Ito, O.; Sasaki, Y.; Yoshikaw, Y.; Watanabe, A. *J. Phys. Chem*. **1995**, *99*, 9838. (b) Sasaki, Y.; Yoshikaw, Y.; Watanabe, A. Ito, O. *J. Chem. Soc., Faraday Trans*. **1995**, *91*, 2287. (c) Ito, O.; Sasaki, Y.; El-Khouly, M. E.; Araki, Y.; Fujitsuka, M.; Hirao, A.; Nishizawa, H. *Bull. Chem. Soc. Jpn*. **2002**, *75*, 1247.

(8) (a) Alam, M. M.; Watanabe, A.; Ito, O. *J. Photochem. Photobiol.; A* **1997**, *104*, 59. (b) Alam, M. M.; Watanabe, A.; Ito, O. *Bull. Chem. Soc. Jpn*. **1997**, *70*, 1833. (c) Alam, M. M.; Ito, O.; Sakurai, N.; Moriyama, H. *Res. Chem. Intermed*. **1999**, *25*, 323.

(9) (a) Nojiri, T.; Alam, M. M.; Konami, H.; Watanabe, A.; Ito, O. *J. Phys. Chem. A* **1997**, *101*, 7943. (b) Nojiri, T.; Watanabe, A.; Ito, O. *J. Phys. Chem. A* **1998**, *102*, 5215. (c) El-Khouly, M. E.; Araki, Y.; Fujitsuka, M.; Ito, O. *Phys. Chem. Chem. Phys*. **2002**, *4*, 3322.

(10) Samanta, A.; Kamat, P. V. *Chem. Phys. Lett*. **1992**, *199*, 635.

(11) (a) Siebrand, W. *J. Chem. Phys*. **1967**, *47*, 2411. (b) Hoytink, G. J. *Acc. Chem. Res*. **1969**, *2*, 114. (c) Gijzeman, O. L. J.; Kaufman, F.; Poter, G. *J. Chem. Soc., Faraday Trans. 2* **1973**, *95*, 9130. (d) Kuzmin, V. A.; Tatikolov, A. S. *Chem. Phys. Lett*. **1978**, *53*, 606. (e) Goudsmit, G.-H.; Paul, H.; Shushin, A. *J. Phys. Chem. A* **1993**, *97*, 13243. (f) Kobori, Y.; Takeda, K.; Tsuji, K. Kawai, A. Obi, K. *J. Phys. Chem. A* **1998**, *102*, 5160. (g) Blank; A.; Levanon, H. *J. Phys. Chem. A* **2001**, *105*, 4799. (h) Kawai, A.; Shikama, A.; Mitsui, M.; Obi, K. *Bull. Chem. Soc. Jpn*. **2001**, *74*, 1203.

(12) Ullman, E. F.; Osiecki, J. H.; Boocock, D. G. B, Darcy, R. *J. Am. Chem. Soc*. **1972**, *94*, 7049.

(13) (a) Konishi, T.; Fujitsuka, M.; Ito, O.; Toba, Y.; Usui, Y. *J. Phys. Chem. A* **1999**, *103*, 9938. (b) Matsumoto, K.; Fujitsuka, M.; Sato, T.; Onodera, S.; Ito, O. *J. Phys. Chem. B* **2000**, *104*, 11632. (c) Onodera, H.; Araki, Y.; Fujitsuka, M.; Onodera, S.; Ito, O.; Bai, F.; Zheng, M.; Yang, J.-L. *J. Phys. Chem. A* **2001**, *105*, 7341.

(14) Scaiano, J. C. *Chem. Phys. Lett*. **1981**, *79*, 441.

(15) Rehm, D.; Weller, A. *Isr. J. Chem*. **1970**, *8*, 259.

(16) Allemand, P. M.; Koch, A.; Wudl, F.; Rubin, Y.; Diederich, F.; Alvarez, M. M.; Anz, S. J.; Whetten, R. L. *J. Am. Chem. Soc*. **1991**, *113*, 1050.

(17) Hung, R. R.; Grabowski, J. J. *J. Phys. Chem*. **1991**, *95*, 6073.

(18) (a) Tanigaki, K.; Ebbesen, T. W.; Kuroshima, S. *Chem. Phys. Lett*. **1991**, *185*, 189. (b) Gevaert, M.; Kamat, P. V. *J. Phys. Chem*. **1992**, *96*, 9883. (c) Ghosh, H. N.; Pal, H.; Sapre, A. V.; Mittal, J. P. *J. Am. Chem. Soc*. **1993**, *115*, 11722.

(19) (a) Park, J.; Kim, D.; Suh, Y. D.; Kim, S. K *J. Phys. Chem*. **1994**, *98*, 12715. (b) Watanabe, A.; Ito, O. Saito, H. Watanabe, M. Koishi, M. *J. Chem. Soc., Chem. Commun*. **1996**, 117.

(20) Steren, C. A.; von Willigen, H.; Biczok, L.; Gupta, N.; Linschitz, H. *J. Phys. Chem*. **1996**, *100*, 8920.

(21) Murov, S. L.; Carmichael, I.; Hug, G. L. *Handbook of Photochemistry*, 2nd ed.; Marcel Dekker: New York, 1993.

(22) Alam, M. M.; Sato, M.; Watanabe, A.; Akasaka, T.; Ito, O. *J. Phys. Chem. A* **1998**, *102*, 7447.

(23) Watanabe, T.; Honda, K. *J. Phys. Chem. A* **1982**, *86*, 2617.